LBL-12102 Rev.
Preprint

Lawrence Berkeley Laboratory
UNIVERSITY OF CALIFORNIA

Materials & Molecular
Research Division

Submitted to the Journal of the Electrochemical Society

ELECTROCHEMICAL STUDIES OF THE FILM FORMATION ON LITHIUM IN PROPYLENE CARBONATE SOLUTIONS UNDER OPEN CIRCUIT CONDITIONS

Y. Geronov, F. Schwager, and R.H. Muller

June 1981

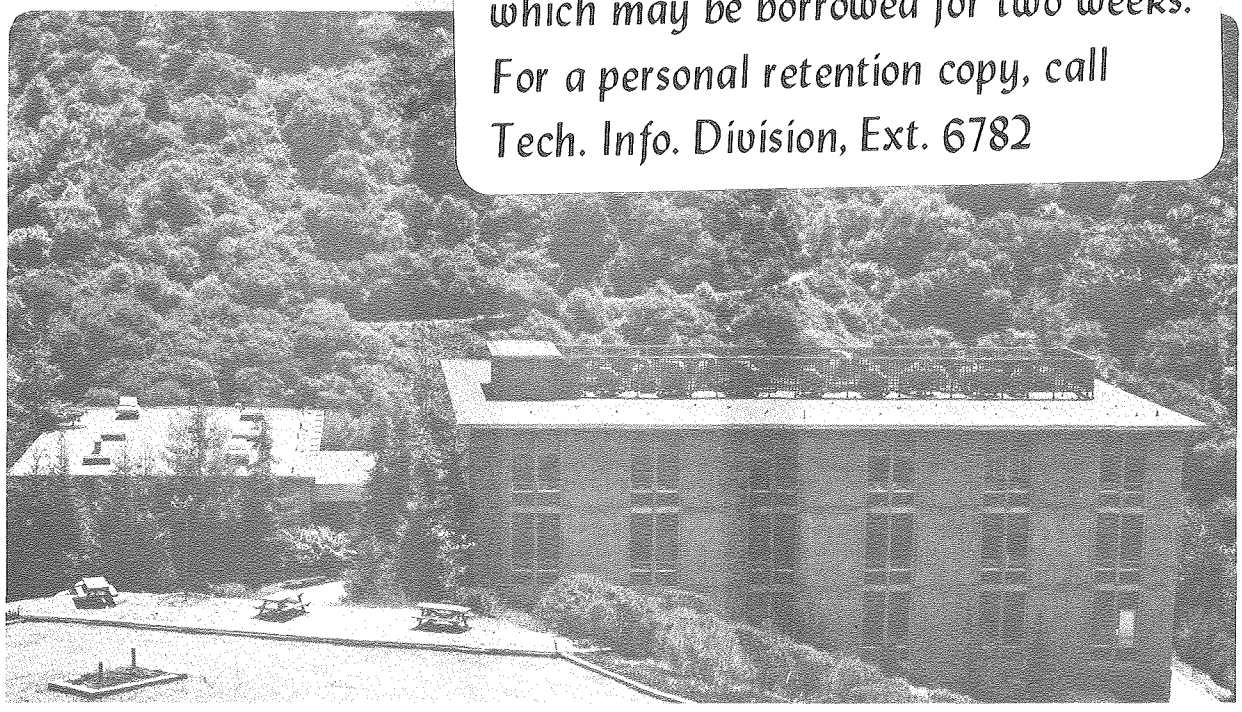

Prepared for the U.S. Department of Energy under Contract W-7405-ENG-48

DISCLAIMER

LBL-12102 - Rev.

Electrochemical Studies of the Film Formation on Lithium in Propylene Carbonate Solutions under Open Circuit Conditions

Y. Geronov,* F. Schwager, and R.H. Muller

Materials and Molecular Research Division
Lawrence Berkeley Laboratory
University of California
Berkeley CA 94720

June 1981

Abstract

The nature of protective surface layers formed on lithium in propylene carbonate solutions of $LiClO_4$ and $LiAsF_6$ at open circuit has been investigated by electrochemical pulse measurements. The results are consistent with the fast formation of a compact thin layer resulting from the reaction with residual water. This layer acts as a solid ionic conductor. Slow corrosion processes produce a thicker porous overlayer.

This work was supported by the Assistant Secretary for Conservation and Renewable Energy, Office of Advanced Conservation Technologies, Electrochemical Research Division of the U.S. Department of Energy under Contract No. W-7405-ENG-48.

---

*Permanent address: Central Laboratory of Electrochemical Power Sources, Bulgarian Academy of Sciences, Sofia, Bulgaria.

Lithium is thermodynamically unstable in contact with most nonaqueous battery electrolytes and can be used only because of the formation of protective films on the metal [1]. It is now generally assumed [2-5] that in most cases the rate-determining step (rds) of the dissolution-deposition process of alkali metals in nonaqueous solutions is not the electron charge transfer but the migration of cation lattice defects through the surface layer. Properties of films on Li in propylene carbonate (PC) solutions have been shown to affect the cycling efficiency of secondary Li electrodes [6,7]. Alloying with an aluminum substrate has been found to be beneficial [8]. On the basis of SEM observations, Dey [1] has derived the formation of an "extremely thin" Li_2CO_3 layer on Li on PC. The same author, as well as Peled [3], has used the previous data of Scarr [9] dealing with the dual Tafel behavior of Li in PC solutions in order to support his assumption of the existence of a surface layer and its influence on the electrode kinetics. Scarr had analyzed his experimental results by means of the Butler-Volmer equation.

The aim of this study is to investigate the kinetics of film formation on lithium in propylene carbonate solutions with different solutes and to determine some film characteristics such as resistance, conductivity, and thickness.

Two principal ways of investigating these problems were chosen: electrochemical (galvanostatic pulse techniques) and optical (ellipsometry). This paper is dealing mainly with electrochemical measurements, while the results from ellipsometry will be presented

separately. The basic assumption of this study is that lithium in PC is covered by a dense surface layer. It acts as an Li-conducting solid electrolyte [6] with no electronic conductivity and has been called Solid Electrolyte Interphase (SEI) [3]. The capacitance across this film is assumed to be electrically connected in series with that of the electrolytic double layer.

The electrochemical behavior of SEI electrodes will be governed by the properties of the SEI. When the SEI is thick enough, the migration of ions through it may be the rate-determining step. In this case it is possible to use the basic equation of the classical theory of ionic conduction in solids developed by Frenkel, Varwey, Cabrera, Mott, and Young [10]:

$$i = 4q\nu\, Fan_{+} \exp(-W/RT) \sinh(aqFE/RT), \qquad (1)$$

where i is the current density, q the charge of the mobile ion, ν the vibration frequency, W the barrier energy, a the half-jump distance, and E the electric field strength. At high electric fields, Eq. (1) can be simplified to:

$$i = i_0 \exp(BE) = i_0 \exp(B\,\eta/Y)\ , \qquad (2)$$

where i_0 is the zero-field ionic current density, B is the field coefficient, η is the potential difference across the film, and Y is the film thickness. Equation (2) represents a Tafel-like polarization dependence.

From this equation a Tafel slope, b, which increases with the film thickness, is obtained:

$$b = 2.3\ Y/B. \tag{3}$$

For low electric fields Eq. (1) reduces to Ohm's law:

$$i = \kappa\ \eta/Y, \tag{4}$$

where κ is the specific conductivity of the SEI. The reaction resistance R_p of an electrode is defined as:

$$R_p = (\eta/i)_{\eta \to 0}. \tag{5}$$

Thus:

$$R_p = 1/\kappa \times Y. \tag{6}$$

When the field strength tends to be zero, one obtains from Eq. (1):

$$(i)_{E=0} = i_o BE. \tag{7}$$

Ohm's law is then applicable and Eqs. (4) and (7) result in:

$$\kappa = (\partial i/\partial E)_{E=0} = i_o B, \tag{8}$$

where i_o is the extrapolated zero-field ionic current density.

Experimental

An electrochemical cell was built to make simultaneous electrochemical and ellipsometric measurements in situ. Clean, optically smooth lithium electrodes were prepared and inserted into the cell in inert atmosphere by pressing 3 mm thick, 5 cm^2 round lithium discs (Foote Mineral, high purity, scraped with a blade) on a polycarbonate foil (cleaned with hexane, alcohol, boiling water (1h), steam (2-3h), and dried in vacuum at 90-100°C) in a special jig. The cross section of a 3.2 mm diameter freshly extruded Li wire, positioned 1 mm from the periphery of the test electrode, served as reference electrode. Two types of solutions were used:

(a) propylene carbonate - $LiClO_4$

(b) propylene carbonate - $LiAsF_6$

Propylene carbonate (Burdick and Jackson, Muskegon MI 49442; distilled in glass) was distilled in a low-pressure distillation column under He atmosphere. The reflux ratio was between 60 and 100, and the head temperature was 145°C. Gas chromatographic analysis showed the water content to be always below 50 ppm. $LiClO_4$ (Alfa p.a.) was dried under vacuum (4-5 mm Hg) at 220°C for 48-73 hours. $LiAsF_6$ (Alfa p.a.) was dried under vacuum at ambient temperature for 7-8 days.

The solutions with 0.05 and 0.1 percent H_2O were prepared by adding water into PC. The solutes were dissolved in the above solutions. In order to avoid any possible reaction of PC vapor with the lithium surface before contact with the liquid, different glove boxes were used for the preparation of electrodes and solutions.

The delay in electrochemical measurements from the moment of electrode scraping was up to 30–45 minutes; the delay after electrolyte filling was 15–30 seconds. Film formation under open-circuit conditions was followed by periodic determinations of electrode capacitance and polarization resistance $R_p = (\partial\eta/\partial i)_{\eta=0}$ by means of the galvanostatic pulse polarization technique. The transients were recorded with a Tektronic 5111 storage oscilloscope, equipped with a Tektronix C-50 camera. A 214B Hewlett Packard pulse generator was used either through a high resistance or through a potentionstat with 2 μs rise time (PAR-371).

The capacitance was derived from the initial slope of short η–t transients (5–10 μs). Anodic and cathodic pulses produced the same results. The steady-state IR-free overpotential values for the determination of R_p were obtained from oscilloscopic traces with a duration of up to 20 ms. To avoid damage to the film, pulses with the smallest possible electric charge were applied.

Results and Discussion

1. Film Thickness

The thickness Y of the film formed during contact of the lithium electrode with propylene carbonate solutions has been derived from the capacitance measurements by use of the formula for two capacitors connected in series [3,4]

$$Y = \sigma\varepsilon/0.113C - Y' \varepsilon/\varepsilon' [\text{Å}] \qquad (9)$$

where ε is the dielectric constant of the lithium film $\varepsilon' = 65$ that of PC, C is the capacitance of the electrode in $\mu F/cm^2$, and σ is the roughness factor, which is assumed to be unity. The thickness Y' of the Helmholtz layer in concentrated electrolytes can be approximated by the length of the dipole (ca. 5 Å for PC); the second right-hand term in Eq. (9) can therefore be neglected. In order for Eq. (9) to be used, the film dielectric constant and the film morphology should be known.

(a) Dielectric constant of film material. According to Dey [1] and Dousek et al. [11], PC reacts with Li to form Li_2CO_3. On the other hand, Butler et al. [12] have demonstrated the predominant role of small amounts of water in the kinetics of fresh Li surfaces. Dousek et al. have pointed out the lack of any decomposition reaction on the bulk Li surface, and even a drastically decreasing rate of PC decomposition on Li amalgam at only 45 ppm H_2O in the PC-$LiClO_4$ solution. Recently, Epelboin et al. [13] have claimed, by ESCA analysis, that PC leads to a chemical formation of a polymeric membrane on the Li substrate.

Investigation of the composition of the films formed on Li in different PC solutions by Auger spectroscopy has so far been inconclusive (see Par. 8b). For the calculation of film thickness from pulse measurements a dielectric constant of 5 was used. This value is close to that of Li_2CO_3 [14]. But one should keep in mind that, for example, at $\varepsilon = 10$ (which is close to the value of 8.9 for Li_2O [15]) the film thickness will double, which in general does not change the present considerations.

(b) Morphology of film. The primary passive film formed on Li in $SOCl_2$ - $LiAlCl_4$ solutions has recently been shown to be dense and pore-free. The porosity of films formed in pure propylene carbonate solutions (120 hrs) was investigated by immersion into solutions of different conductivity (0.15M and 1.0M $LiClO_4$/PC). The electrode capacitance and polarization resistance were found to be the same for both solutions and did not change during two days ($C = 0.14 \pm 0.02$ $\mu F/cm^2$ and $R_p = 380 \pm 20$ ohm cm^2). This result is evidence for the absence of electrolyte-filled pores in the film which controls the pulse measurements.

As will be shown further, higher water amounts in the PC solutions increase the probability of a secondary porous film formation. The porous film does not possess protective properties and presumably would influence to a negligible extent the passive behavior of lithium in PC solutions, since the passivity of Li is governed by the primary nonporous film. Data for the primary passive film measured after up to 5 days of storage were considered more accurate because the porous film is not yet very thick or dense.

2. High-Field Experiments

The steady-state IR-free overpotential values were calculated from the transients in the range of current densities between 0.050-20 mA/cm^2. At the higher current densities (i.e., higher electric fields, above about 10^6 V/cm), a Tafel-like polarization dependence is expected [Eq. (2)]. Figure 1 presents a series of Tafel

plots obtained by the pulse technique after 0 to 6 days' immersion, resulting in different film thicknesses. As required for a field-assisted ion current across an insulating film, the Tafel slope, b, increases with film thickness. The extrapolated lines intersect at zero overpotential at the zero-field current density, $i_0 = 3$ mA/cm^2.

Curve 1 of Fig. 1 was obtained a few minutes after electrolyte filling. The value of the zero-field current density i_0 of 5.5 mA/cm^2 obtained by this plot can be compared to exchange currents reported by other authors in terms of the electron transfer reaction mechanism. For example, Butler et al. [12] have reported an extrapolated value of the exchange current in 0.001 M H_2O/PC/$LiClO_4$ on freshly cut Li surface of 12 mA/cm^2. An exchange current of 3.3 mA/cm^2 was reported by Epelboin et al. [13] by using anodic polarization techniques for surface cleaning. The value of 5.5 mA/cm^2 obtained in this study for the specularly reflecting Li surface coincides well with the value of 12 mA/cm^2 [12] for a roughness factor of 2 to 3 given by the previous authors [13]. This is evidence for comparable cleanliness of the Li surfaces used in both studies.

This higher value of i_0 obtained just after immersing the electrode, as compared to the zero-field current (2.7-3.0 mA/cm^2), suggests that immediately after electrode immersion into the solution the electrode charge-transfer step is rate determining.

The electrode capacitance of 1.3-1.6 μF/cm^2 is lower than that of the double layer which supports the presence of a film of 15-30 Å (ϵ = 5-10) at the time of immersion.

The value of the field coefficient B (Eq. (3)) may be obtained from the slopes b-Y plot presented in Fig. 2. This value, $B = 1.2 \pm 0.1 \times 10^{-6}$ cm/V, is very close to that of typical barrier films [10].

Plots of log i - E in different solutions are given in Fig. 3. It is found that the current density does not depend on the film thickness. This finding supports the assumption of the rate-determining step being the ion migration through the film. From the plot log i - E, using Eq. (2) the value of B can also be determined. It can be seen that adding water to $LiClO_4$ solutions decreases the field coefficient, B (slope, Eq. (2)). For $LiAsF_6$ solutions, the field coefficient is larger ($1.8 \pm 0.1 \times 10^{-6}$ cm/V). The zero-field current density is the same for the three solutions ($2.9 \pm 0.2 \times 10^{-3}$ A/cm^2), indicating similar film properties in different media. These values of B and i_o were used to calculate the specific conductivity of the film by the low-field approximation, Eq. (8), resulting in
$(3.1 \pm 0.25) \times 10^{-9}$ ohm^{-1} cm^{-1} for $LiClO_4$ solutions and
$(5.1 \pm 0.2) \times 10^{-9}$ ohm^{-1} cm^{-1} for $LiAsF_6$ solutions.

Experimentally found values of the Tafel slope, b, at different film thicknesses can be derived from Fig. 1. As has been seen from Eqs. (1)-(3), the Tafel slope is equal to

$$b = 2.3\ RT\ Y/aqF. \qquad (10)$$

For $q = 1$ and $a = 3$ Å, this formula is simplified to

$$b(mV) = 20\ Y \qquad (11)$$

A comparison between the experimental and theoretical values of b is given in Table I. If one considers that other combinations of dielectric constant ϵ and half-jump distance a of the film could be used, the agreement of measured and computed Tafel slopes (for $\epsilon = 5$ and $a = 3$ Å) is satisfactory.

3. Low-Field Experiments

Figures 4 and 5 present typical sets of experimental plots reflecting the increase of the electrode resistance R_p and the reciprocal capacitance 1/C with time for Li electrodes immersed in PC/$LiClO_4$ and PC/$LiAsF_6$ solutions, respectively. It was found in more than 30 experiments that all 1/C – R plots intersect the same point with the coordinates: $1/C = 0.70 \pm 0.10$ $cm^2/\mu F$ and $R = 8 \pm 2$ ohm cm^2. This observation supports the existence of a capacitance connected in series with the capacitance across the passive film. This capacitance is low compared to that of the Helmholtz double layer (10–20 $\mu F/cm^2$) [8,12,13], and probably it is a capacitance of a surface layer formed in the glove box [16].

Hence the thickness of the film formed during the contact of lithium with the solution can be calculated from Eq. (12) instead of Eq. (9):

$$Y = 8.85 \times 10^{-8} \varepsilon\sigma \, (1/C - 1/C_d)[cm] \qquad (12)$$

where C is the film capacitance and C_d is the intersection of the plot $(1/C - R_p)$ with the 1/C ordinate (actually this involves an error of a few Å if, instead of R_p = 5-8 ohm cm^2, R_p = 20 is taken).

From the slope of $1/C - R_p$, using Eqs. (6) and (12), the values of specific conductivity of the primary passive film in different PC solutions can be derived. This value for PC/$LiClO_4$ solutions is $2.7 \pm 0.2 \times 10^{-9}$ ohm^{-1} cm^{-1} (Fig. 4) and for PC/$LiAsF_6$ - $5.1 \pm 0.25 \times 10^{-9}$ $ohm^{-1}cm^{-1}$ (Fig. 5). Both are very close to the value of κ, estimated from the low-field approximation [Eq. (8)].

4. Effect of Water

Figure 6 presents the change of the electrode resistance during the time of storage. In the same figure, curves 1 and 2 are for 0.5M $LiAsF_6$ solutions with 20 and 1000 ppm H_2O, respectively, and curves 3, 4, and 5 are for 0.5M $LiClO_4$ solutions with 20, 500, and 1000 ppm H_2O, respectively. The curves show that the rate of film formation increases with water concentration. This trend is much stronger in PC/$LiClO_4$ solutions than in $LiAsF_6$.

From Fig. 5 it can also be seen that there is no difference between the conductivity of films formed in PC/0.5M $LiAsF_6$ with 20 ppm H_2O and those with 1000 ppm H_2O. On the other hand, the film conductivity in $LiAsF_6$ solutions is always higher than in $LiClO_4$

solutions independent from the water concentration. For example, from the lower two curves in Fig. 4, one calculates values of 0.8 to 1.5×10^{-9} cm^{-1} ohm^{-1} for κ for $LiClO_4$ solutions with 500–1000 ppm H_2O. The corresponding value for $LiAsF_6$ solutions (Fig. 5) is 4–7 times lower. The former values are 2–3 times lower than the conductivity of passive films formed in $LiClO_4$ solutions with 20 ppm H_2O ($2.5–3.5 \times 10^{-9}$ ohm^{-1} cm^{-1}).

The same tendency of thin-film conductivity change is also demonstrated from the high-field experiments (see Fig. 3), but to a lesser extent. For example, the expected field coefficient, B, for PC/0.5M $LiClO_4$ solutions with 1000 ppm of water should be approximately two times lower in order to fit the calculated value of specific conductivity according to Eq. (8)($\kappa = i_o B$) to that obtained from low-field experiments (Fig. 4). This disagreement, found only in PC/$LiClO_4$ solutions of high water content, is probably due to some influence of the secondary porous film. On the other hand, it is noteworthy that the Tafel plots log i – E taken from the passivated lithium electrode in pure PC, PC with 0.5M $LiAsF_6$, and PC/$LiAsF_6$ with 1000 ppm H_2O show the same slope, the same field coefficient $B = 1.8 \times 10^{-6}$ V^{-1} cm, and zero current density $i_o = 2.7 \times 10^{-3}$ A/cm^2 (Fig. 7). The specific conductivity calculated using these values of B and i_o is very close to the one found for $LiAsF_6$ solutions from low-field experiments (see Fig. 5), 4.9×10^{-9} ohm^{-1} cm^{-1}.

This observation supports the following ideas: (a) passive layers are formed the same way in PC without any salt and with $LiAsF_6$ as solute, (b) $LiAsF_6$ does not take part in the film formation, and (c) film is formed as a result of reaction of Li with water impurity. The last suggestion is reinforced by the increase of the rate of formation with increasing water concentration.

A very surprising result from this set of experiments was that lithium corroded faster in PC (without salt) containing 0.1 percent H_2O than in solutions of $LiClO_4$ and $LiAsF_6$ with the same amount of water. After seven days storage in this solution, a lithium mirror-like bright surface turns dark grey. This has never happened in the solutions with $LiClO_4$ or $LiAsF_6$ with the same water concentrations. Electron micrographs (Figs. 13,15) also illustrate this difference. The water activity appears to be reduced by the presence of salts.

So far, there is no reasonable explanation for the decrease in film conductivity with increasing water content of $LiClO_4$ solutions. However, the fact that even in $LiClO_4$ solutions with low H_2O concentration the film conductivity is always lower than in $LiAsF_6$ solutions and pure PC suggests the important role of $LiClO_4$ in the film formation.

5. Effect of Cathodic Pulse Polarizations

The overpotential behavior of the Li electrode in $PC/LiClO_4$ was found to be different for anodic and cathodic polarization. In Fig. 8, the difference between cathodic and anodic overpotentials, $\Delta\eta$, is related

to the film thickness for 0.5 mA/cm^2 and 1 mA/cm^2 current pulses of 10 ms duration.

The higher overpotential (or higher resistance) of the process of the Li deposition in $LiClO_4$ can be attributed to the difficulty of the Li^+ transport across the solution/film or the film/metal interfaces. In PC/$LiAsF_6$ solutions completely symmetric behavior was observed up to 15 mA/cm^2. A similar effect of asymmetric overpotential behavior of magnesium electrodes in $SOCl_2$ solutions was reported by Peled and Strase [17]. They explained the effect as being due to the rather difficult process of solvated molecules shedding their solvent before entering the passivating layer. The dependence of the excess cathodic voltage $\Delta\mu$ on film thickness (Fig. 8) is, however, not consistent with solvent molecule shedding at the solution/passive layer interface.

6. Film Growth

As it was recently demonstrated [18], a good agreement with experimental results of the passive film growth in $SOCl_2$ - $LiAlCl_4$ solutions can be obtained if an additional slow film corrosion is taken into account. The corrosion rate is assumed to rule the growth of the secondary porous film in the postulated dual-film model.

The same approach is used in this study, especially for solutions containing 0.05 and 0.1 percent H_2O where the corrosion rate is higher. The equations used are:

$$v = (\partial Y/\partial t) = v_g - v_c \tag{13}$$

$$v = \Delta\phi V_m \kappa/YF - v_c \tag{14}$$

$$v = A/Y - v_c \ [cm/s]. \tag{15}$$

Here v is the instantaneous net rate of film growth calculated by graphical differentiation of the Y-t curves, v_g is the rate of the primary passive film growth by field-assisted ionic migration in the solid phase, v_c is the rate of corrosion assumed to be independent of film thickness and time, $\Delta\phi$ is the potential difference in the film, V_m is the molar volume of the passive film in cm^3/mole, and κ is the specific conductivity of the film.

In Fig. 9, v is plotted vs the reciprocal film thickness 1/Y. The slopes of the plot v vs 1/Y yield the kinetic constant, A, the intercept with the abscissa gives a steady-state thickness Y_∞ for v = 0. Under this condition, Eq. (15) yields the corrosion rate of the film

$$v_c = A/Y_\infty \ [cm/s]. \tag{16}$$

Table II presents the kinetic data obtained from the plots in Fig. 9. For comparison, data on Li in $SOCl_2/LiAlCl_4$ are also included [18].

Film growth rates derived from simultaneous ellipsometric measurement in the same solutions [19] are of the same order of magnitude

as those presented in Table II. For example, ellipsometry gives for v_c in PC/1M $LiClO_4$ solution with 0.1 percent H_2O a value of $0.15\text{–}0.3 \times 10^{-12}$ cm/s, assuming a constant growth of the porous film during 10 days of storage.

Corrosion rates of Li in PC solutions can be seen to be two orders of magnitude lower than in $SOCl_2$ - $LiAlCl_4$ solutions.

7. Temperature Dependence

With a dielectric constant of 5, assuming that ε does not depend on the solute and the film density, a field constant B, typical for barrier films, was derived. This value is for PC/$LiAsF_6$ $1.8 \pm 0.2 \times 10^{-6}$ V^{-1} cm, and for PC/$LiClO_4$ solutions 0.8 to 1.3×10^{-6} V^{-1} cm, depending on the water content. This agreement of the experimental results with the basic equation of the ionic transport, and especially the accuracy of the experimentally found thickness used for calculating the kinetic constants, could be determined once more.

Following Young [10], the Eq. (2) $i = i_o \exp(BE)$ is valid when the backward current is negligible compared to the forward current. Hence, the ratio P will indicate this validity:

$$P = \exp -(W - qaE)/\exp -(W + qaE) \qquad (15)$$

where W is the activation (barrier) energy, q is the ion charge of the mobile ion, a is the half-jump distance, and E is the field strength.

The apparent activation energy of the ionic conductivity was assessed by the temperature dependence of κ of the passive film, formed in PC/0.5 m $LiClO_4$ in the temperature range -20 to +20°C. The Arrhenius plot (Fig. 10) yields 0,61 V. This value with a = 3 Å and q = 1e for a field $E = 10^6$ V/cm gives $P \simeq 10$. This means that at electric fields of 10^6 V/cm a Tafel-like behavior is expected. The experimental results summarized in Figs. 3 and 7 have confirmed this theoretical expectation.

8. Surface-Film Observations

(a) Scanning Electron Microscopy (SEM). Electrode surfaces resulting from exposure to pure PC and solutions of $LiClO_4$ and $LiAsF_6$ of different water content have been examined by SEM. The lithium specimens were transferred from the glove box to the SEM in a transfer device under 10-20 μ of helium. Transfer time was about 1 hr. The film morphology was found to depend on the electrolyte composition as well as on storage time. With higher water concentration and longer storage time, a coarser crystalline film with higher porosity was observed. At low water concentration the film formed in $LiClO_4$ appears slightly less porous than that formed in $LiAsF_6$ (Fig. 11). However, nearly the same rough and porous structure was observed in both solutions when the water level was increased to 0.1 percent (Fig. 12).

Li corrosion in propylene carbonate is decreased by increasing the concentration of $LiClO_4$ and $LiAsF_6$ (Figs. 13 and 14).

The microstructure shown by the pictures agrees with the findings in sections 4 and 6 about the importance of electrolyte salts for film growth and corrosion.

The pore-free dense structure obtained in pure PC (Fig. 15) is consistent with electrochemical experiments mentioned before (Sec. 1b). In this study, the porous film was assumed to possess low protective properties, and because of this it influences the investigated Li passivity to a negligible extent. This assumption is probably not valid for longer storage times. Electrochemical measurements on nonporous primary films formed up to six days are not affected by the resistance of a porous overlayer.

(b) Auger Electron Spectroscopy (AES). Auger spectra and depth profiles on Li electrodes stored in different PC solutions have been determined. The most reproducible results were obtained with lithium stored in PC without salt. A 5 min depth profile of Li, C, O (atomic percentages) on electrodes stored for two weeks in pure PC is shown in Fig. 16. If we assume that the bare Li surface is reached after 3 min of sputtering, an approximate film thickness of 400-500 Å is derived from a calibrated sputter rate of 150 Å/min for Ta_2O_5 under the same conditions. This value is of the order of the value of 300-350 Å (0.12-0.14 $\mu F/cm^2$; ε=5). No firm conclusions about the chemical composition of the film could be drawn from the Auger spectra. The carbon content observed is not necessarily due to the presence of Li_2CO_3, but could be caused by residual CO in the UHV-chamber.

9. General Discussion and Conclusions

The present study supports the idea that the stability of Li in PC solutions at open-circuit and ambient temperature can be attributed to the formation of a nonporous ionically conducting and electronically insulating film.

The increase of film formation rate at higher water concentration and the independence of the specific conductivity of the films of the water level in PC-$LiAsF_6$ solutions demonstrate the importance of the reaction of Li with water in propylene carbonate solutions, which is also supported by the SEM observations. Li_2O is the thermodynamically favored reaction product. The importance of water has also been pointed out by Butler et al. [12] and Besenhard and Eichinger [20].

Recently, Froning et al. [16] and Keil et al. [21] have shown that even at extremely low oxygen exposures (66 Langmuirs) the freshly cut Li surface is immediately covered by a Li_2O film. Oxygen exposure of the lithium electrode during preparation in the dry box is larger.

In this study it has been shown that the specific conductivity of the passive film formed in PC/$LiAsF_6$ is two to three times higher than that in PC/$LiClO_4$. Anodic and cathodic overpotentials were found to be symmetric in $LiAsF_6$-solutions, whereas the cathodic overpotential was higher than the anodic in $LiClO_4$-solutions. This is in agreement with findings by Brummer et al. [22] that AsF_6^- improves the Li cycling efficiency in PC solution, probably as a result of the higher conductivity of the film formed in AsF_6^- containing solutions as compared to films from ClO_4^- solutions.

In addition to the nonporous layer responsible for inhibiting the spontaneous reaction of lithium, a nonprotective outer porous film region seems to be formed by a corrosion process. This part of the film does not effect electrochemical measurements but is visible in scanning electron micrographs and is found in ellipsometer measurements.

Acknowledgment

This work was supported by the Assistant Secretary for Conservation and Renewable Energy, Office of Advanced Conservation Technologies, Electrochemical Research Division of the the U.S. Department of Energy under Contract No. W-7405-ENG-48.

This material was presented in part at the Hollywood, Florida, Meeting of the Electrochemical Society, as a Recent Newspaper, No. 706 RNP.

References

1. A.N. Dey, Thin Solid Films 43, 131 (1977).
2. E. Peled and H. Yamin, 18th Power Sources Symposium, 237 (1978).
3. E. Peled, J. Electrochem. Soc. 126, 2047 (1979).
4. R.V. Moshtev, Y. Geronov, B. Puresheva, and A. Nasalevska, 28th ISE Meeting, Varna, Extend. Abstract 153 (1977).
5. A. Leef, A. Gilmour, J. Appl. Electrochem. 9, 663 (1979).
6. R.D. Rauh and S.B. Brummer, Electrochim. Acta 22, 75 (1977).
7. M. Garreau, J. Thevenin, and D. Warin, Progress in Batteries, Vol. 2, JEC Press, Cleveland OH, 1979, p. 54.
8. I. Epelboin, M. Froment, M. Garreau, J. Thevenin, and D. Warin, in Power sources for biomedical implantable applications and ambient temperature lithium batteries, B.B. Owens and N. Margalit, Eds., Vol. 80-4, Electrochemical Society, 1980, p. 417.
9. R.F. Scarr, J. Electrochem. Soc. 117, 295 (1970).
10. L. Young, Anodic oxide films, Academic Press, New York, 1961.
11. F.P. Dousek, J. Jausta, and L. Riha, J. Electroanal. Chem. 46, 281 (1973).
12. J.N. Butler, D.R. Cogley, and J.C. Synott, J. Phys. Chem. 73, 4026 (1969).
13. I. Epelboin, M. Froment, M. Garreau, L. Thevenin, and D. Warin, J. Electrochem. Soc. 127, 2100 (1980).
14. American Institute of Physics Handbook, McGraw-Hill, 1963.

15. Landolt-Bornstein, Vol.II, Part 6, Springer, 1959, p. 455.

16. M.H. Froning, T.N. Wittberg, W.E. Modeman, Abstract 14, Electrochem. Soc. Meeting, Los Angeles CA, October 1979.

17. E. Peled and H. Straze, J. Electrochem. Soc. 124, 1030 (1977).

18. R.V. Moshtev, Y. Geronov, and B. Puresheva, J. Electrochem. Soc., in press.

19. F. Schwager, Y. Geronov, R. Muller, Abstract 3, Electrochem. Soc. Meeting, Hollywood FL, October 1980.

20. J.O. Besenhard and G. Eichinger, J. Electroanal. Chem. 68, 1-18 (1976).

21. R. Keil, J. Hoenigman, W. Modeman, T. Wittberg, and J. Peters, Interim Techn. Report, October 1979. AFWAL-TR-80-2018, Univ. of Dayton Research Inst., Dayton OH.

22. S.B. Brummer, in Proceedings, Workshop on Li Nonaqueous Battery Electrochemistry, E.B. Yeager et al., eds., Electrochemical Society 1980, p. 13.

Table I

Comparison between Experimental and Theoretical Tafel Slopes

Y Å	b_{exp} mV	$b_{theor.}=20Y$ mV
25	460	500
37	670	740
65	1150	1300
103	1840	2060
130	2400	2600
138	2650	2760
162	3255	3240

Table II

Kinetic Data of Film Growth in Different Media

Electrolyte	Y Å	$x10^9$ $ohm^{-1}cm^{-1}$	A cm^2/s	v_c cm/s
PC/0.5M $LiClO_4$, 0.1% H_2O	114	0.81	$1.3x10^{-18}$	$1.15x10^{-12}$
PC/1.0M $LiClO_4$, 0.1% H_2O	167	1.34	$1.8x10^{-18}$	$1.08x10^{-12}$
PC/0.5M $LiAsF_6$, 0.1% H_2O	167	5.3	$4x10^{-18}$	$2.4x10^{-12}$
$SOCl_2$/1M $LiAlCl_4$	200	0.64	$2x10^{-16}$	$1x10^{-10}$

Figure Captions

Fig. 1 Tafel plots at constant film thickness (derived for $\varepsilon = 5$, anodic polarization), 1-25 Å, 2-37 Å, 3-65 Å, 4-103 Å, 5-130 Å, 6-138 Å, 7-162 Å. (XBL 806-10429)

Fig. 2 Relationship between film thickness Y and Tafel slope b. (XBL 8012-13349)

Fig. 3 Tafel plots, log i vs E, in different propylene carbonate solutions, 30-200 Å films: 1-0.5M $LiAsF_6$, 2-0.5M $LiClO_4$, 3-0.5M $LiClO_4$ + 0.1% H_2O. (XBL 809-5972).

Fig. 4 Reciprocal capacitance, 1/C vs polarization resistance, R_p, in the following propylene carbonate solutions: o,●-1M $LiClO_4$, ▽-1M $LiClO_4$ + 0.05% H_2O, ▼-1M $LiClO_4$ + 0.1% H_2O, □ -0.5M $LiClO_4$ + 0.1% H_2O. (XBL 8012-13355)

Fig. 5 Reciprocal capacitance, 1/C vs polarization resistance R_p, in hexafluoroarsenate solutions. ●,o-0.5M $LiAsF_6$, Δ-0.5M $LiAsF_6$ + 0.1% H_2O. (XBL 8012-13354)

Fig. 6 Time-dependence of Li electrode resistance in different propylene carbonate solutions: 1-0.5M $LiAsF_6$; 2-0.5M $LiAsF_6$ + 0.1% H_2O; 3-0.5M $LiClO_4$; 4-0.5M $LiClO_4$ + 0.05% H_2O; 5-0.5M $LiClO_4$ + 0.1 H_2O. (XBL 8012-13352)

Fig. 7 Tafel plots, log i vs E, for: Δ-PC without salt, Y + 307 Å; □-PC/0.5M $LiAsF_6$, Y = 215 Å; o-PC/0.5M $LiAsF_6$ + 0.1% H_2O, Y = 205 Å. (XBL 8012-13350)

Fig. 8 Dependence of the excess voltage, $\Delta\eta$, on the film thickness in 1M $LiClO_4$ at: 1-0.5 mA/cm^2, 2-1 mA/cm^2. (XBL 8012-13353)

Fig. 9 Dependence of the net rate of film growth, v, on the reciprocal film thickness, 1/Y. Propylene carbonate solutions with 0.1% H_2O: 1-0.5M $LiCl)_4$, 2-1.0M $LiClO_4$, 3-0.5M $LiAsF_6$. (XBL 8012-13351)

Fig.10 Temperature dependence of the ionic conductivity through the film on lithium formed in 0.5M $LiClO_4$ solution. (XBL 808-5726)

Fig.11 SEM picture of Li surface after two weeks of storage in 0.5M $LiAsF_6$, 15,000x. (XBB 809-11290)

Fig.12 SEM picture of Li surface after one week of storage in 1M $LiAsF_6$ + 0.1% H_2O, 15,000x. (XBB 811-197)

Fig.13 SEM picture of Li surface after five days of storage in PC with 0.1% H_2O, 1000x. (XBB 800-14890)

Fig.14 SEM picture of Li surface after five days of storage in PC + 0.1% H_2O + 1.2M $LiClO_4$, 2000x. (XBB 800-14892)

Fig.15 SEM picture of Li surface after five days of storage in PC containing 10 ppm H_2O, 15,000x. (XBB 800-14896)

Fig.16 AES depth profile of Li stored for two weeks in propylene carbonate: argon beam V = 3kV, i-15 nA. (XBL 8012-13562)

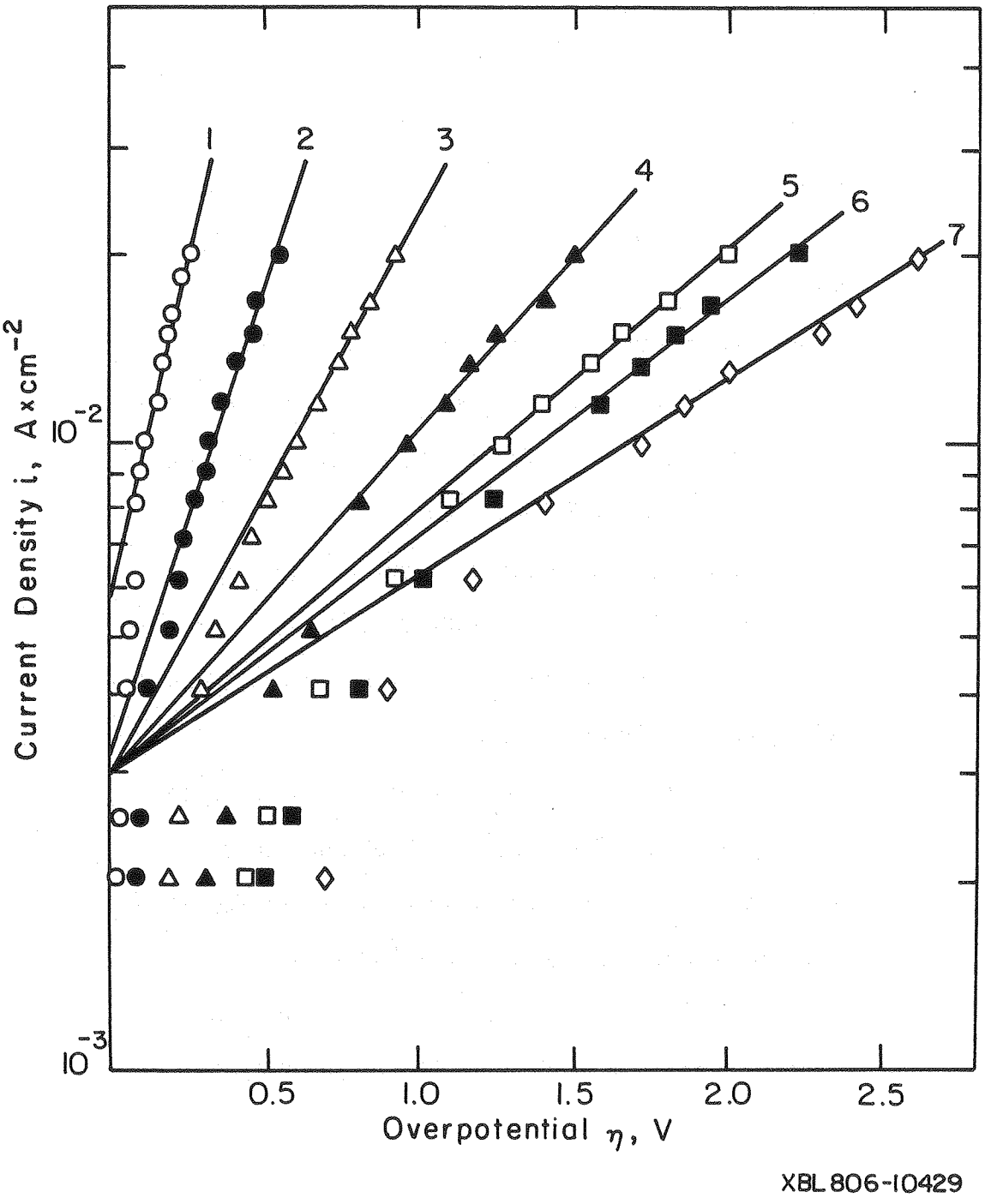
1
2
3
4
5
6
7
Current Density i, A x cm^{-2}
10^{-2}
10^{-3}
0.5
1.0
1.5
2.0
2.5
Overpotential η, V
XBL 806-10429

Figure 1

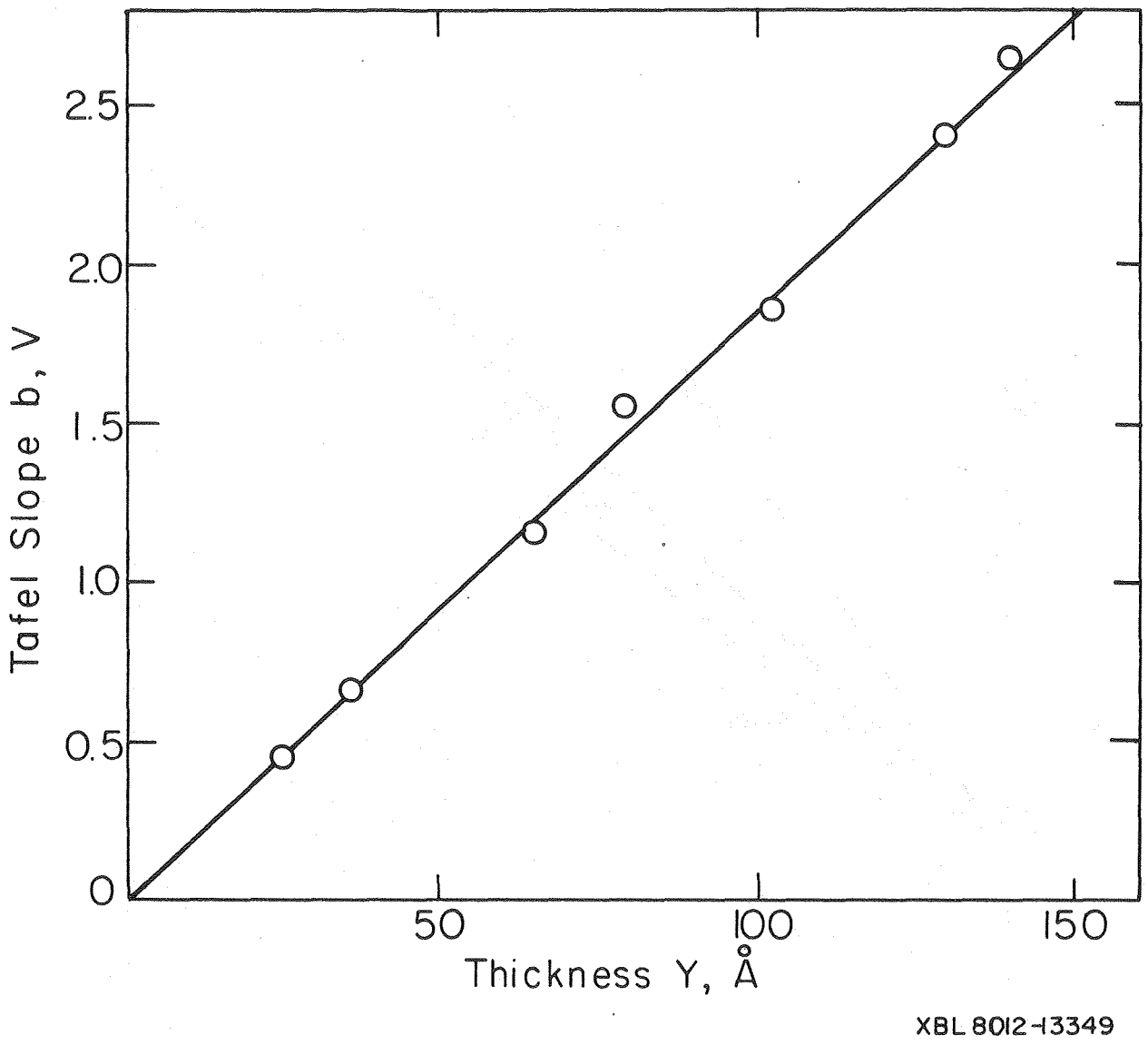
Tafel Slope b, V
2.5
2.0
1.5
1.0
0.5
0
50
100
150
Thickness Y, Å
XBL 8012-13349

Figure 2

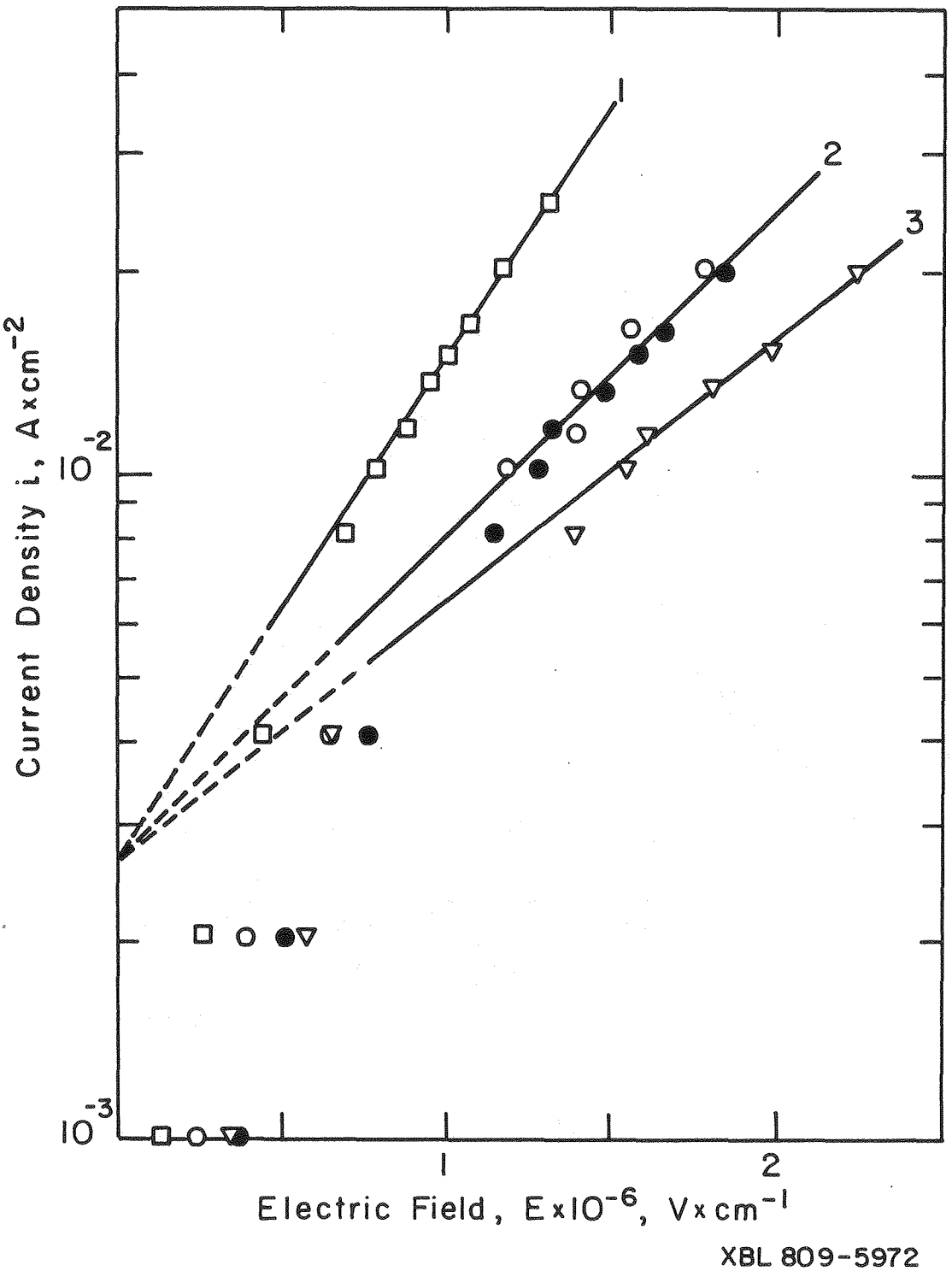
Current Density i, A x cm^{-2}
10^{-2}
10^{-3}
1
2
3
1
2
Electric Field, E x 10^{-6}, V x cm^{-1}
XBL 809-5972

Figure 3

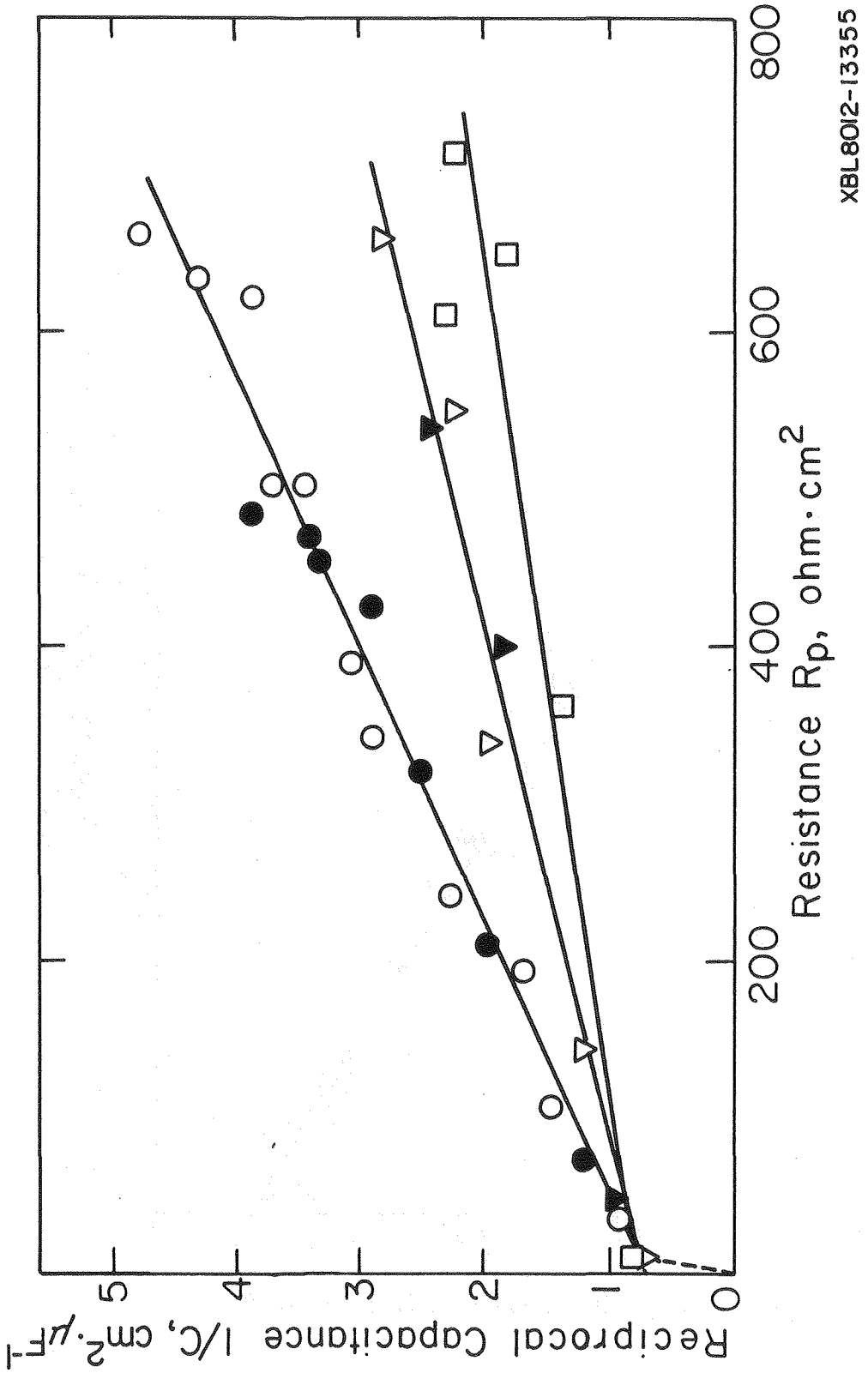
Reciprocal Capacitance 1/C, cm²·μF⁻¹
0
1
2
3
4
5
200
400
600
800
Resistance Rp, ohm·cm²
XBL8012-13355

Figure 4

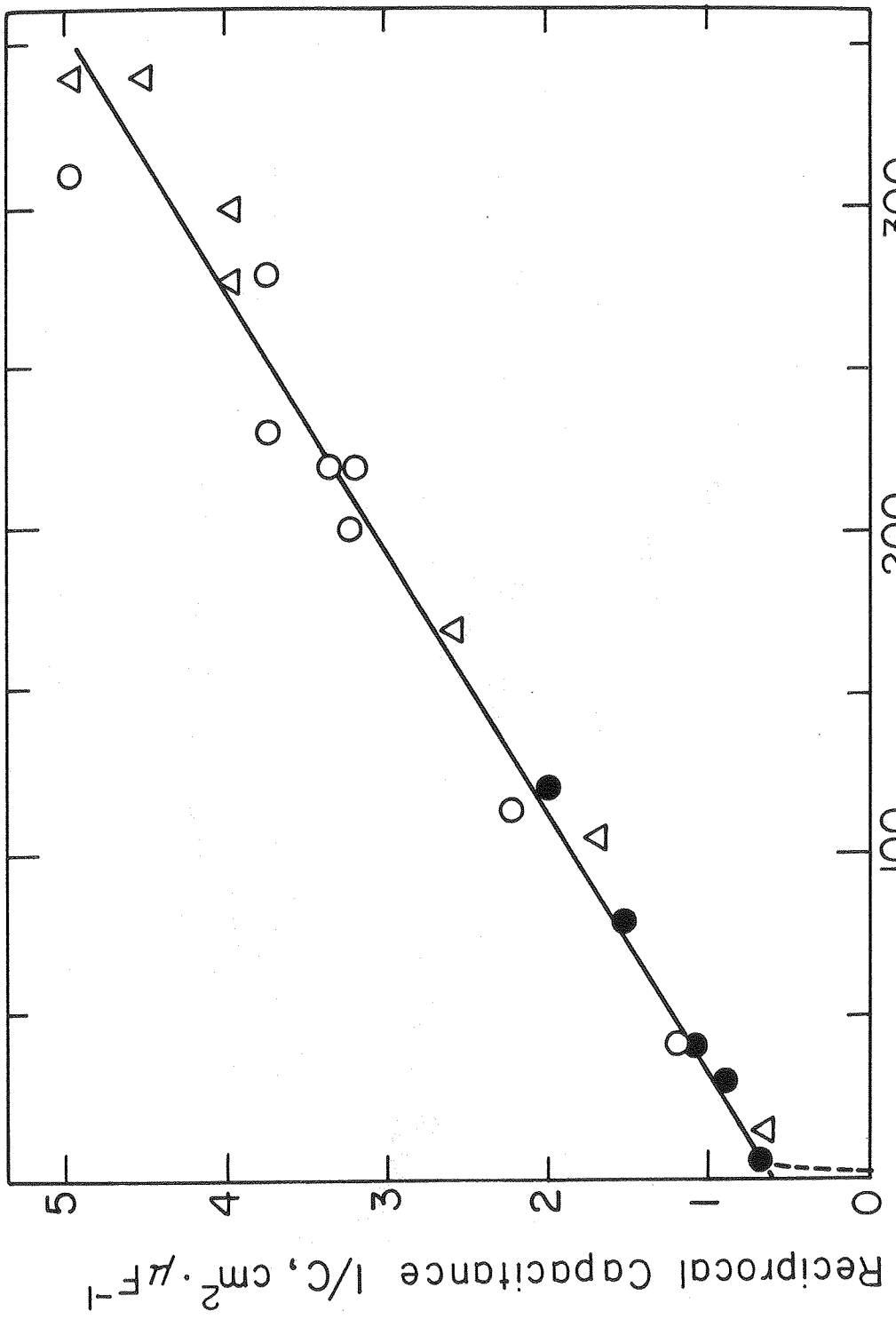

XBL 8012-13354

Figure 5

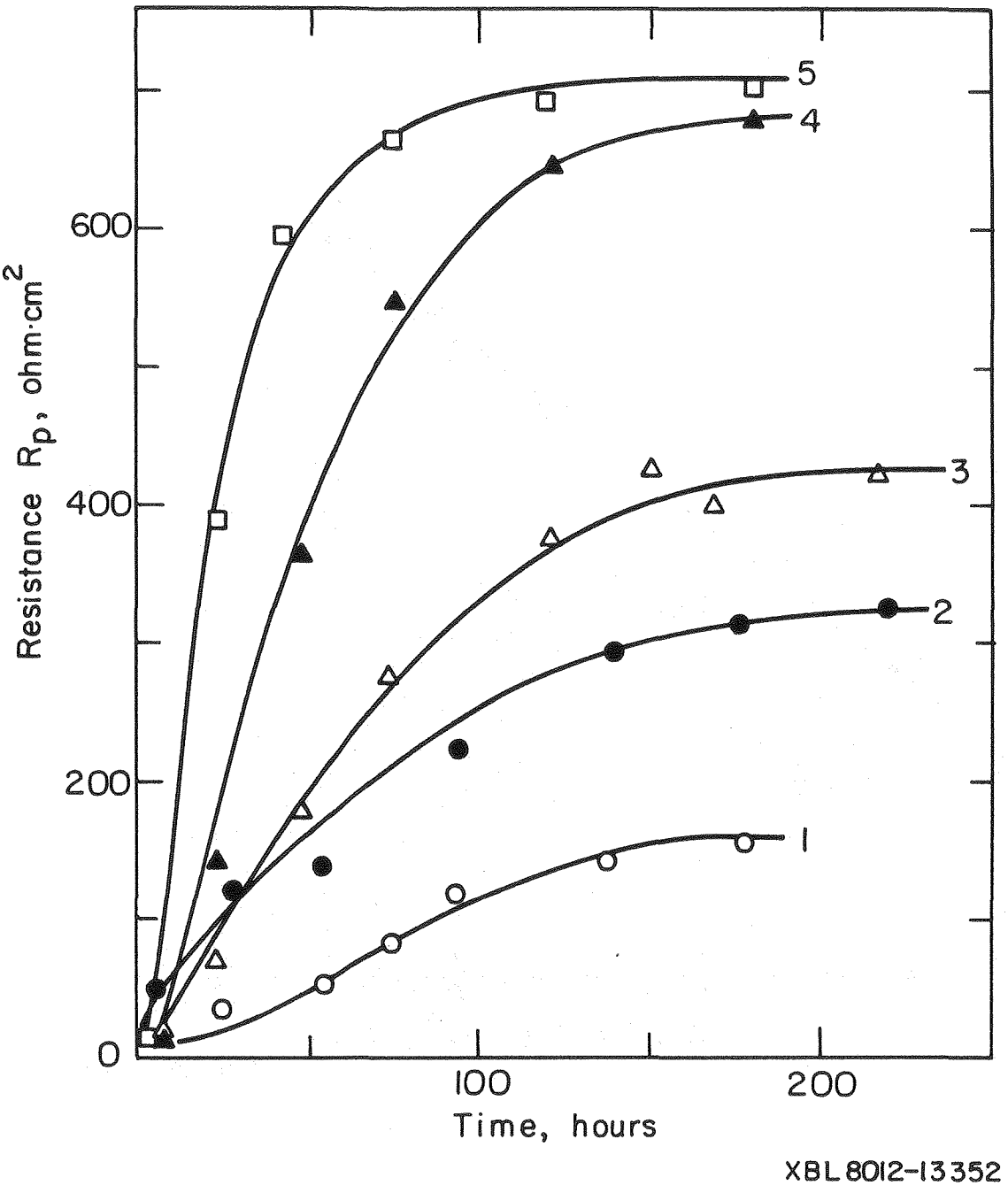
Resistance R_p, ohm·cm^2
0
200
400
600
100
200
Time, hours
1
2
3
4
5
XBL 8012-13352

Figure 6

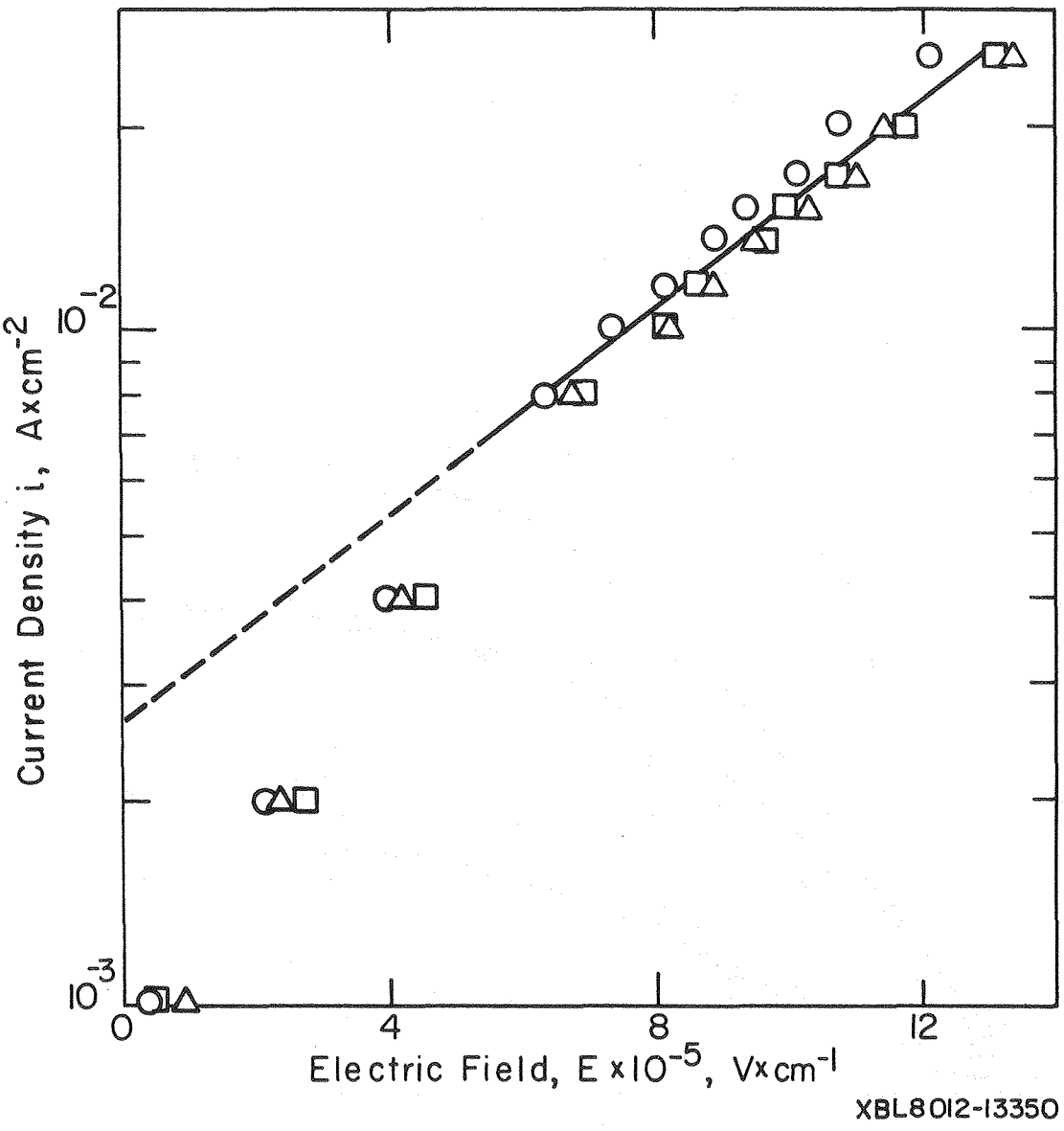
Current Density i, Axcm^{-2}
10^{-2}
10^{-3}
0
4
8
12
Electric Field, E x10^{-5}, Vxcm^{-1}
XBL8012-13350

Figure 7

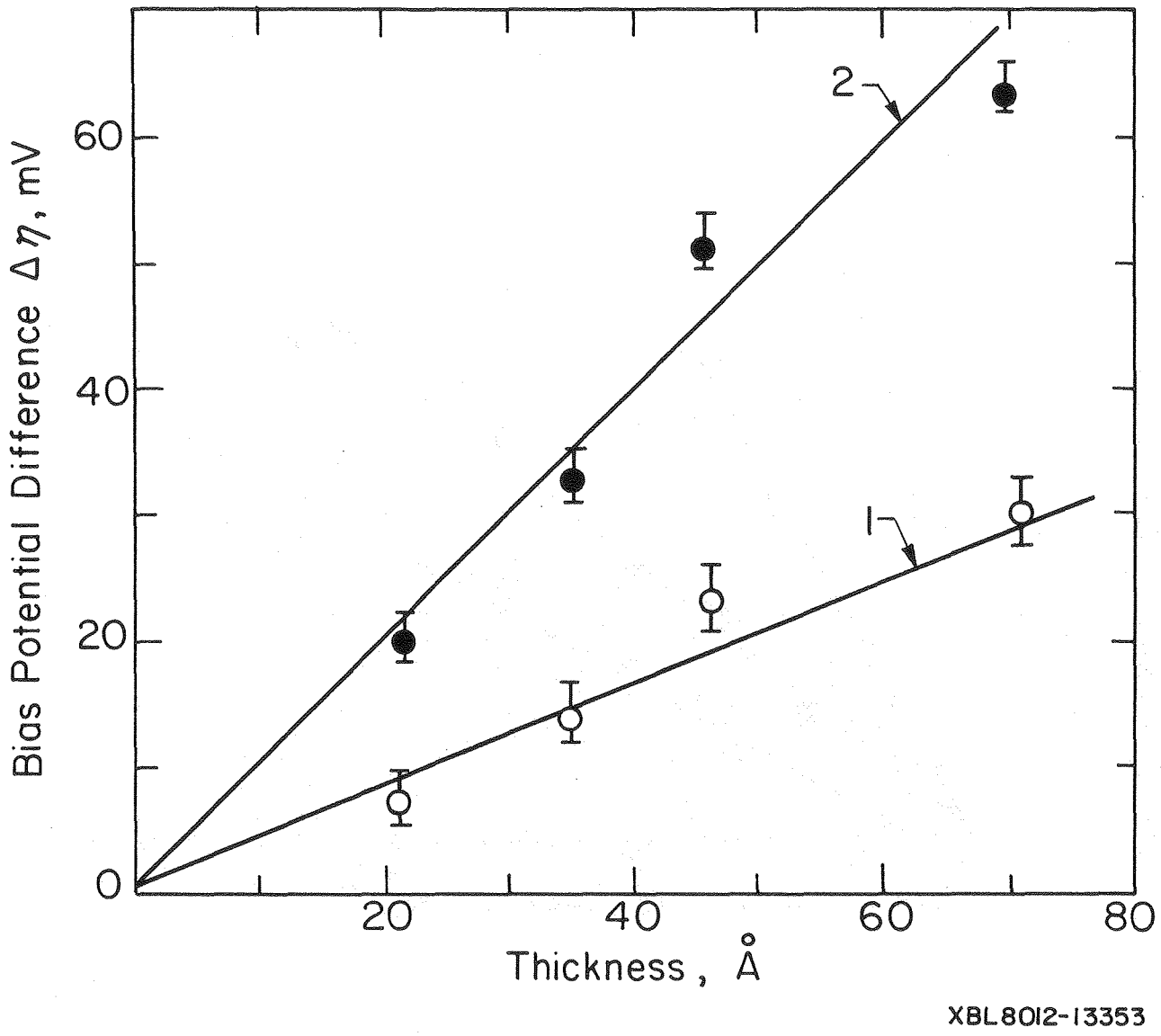
Bias Potential Difference Δη, mV
0
20
40
60
20
40
60
80
Thickness, Å
2
1
XBL8012-13353

Figure 8

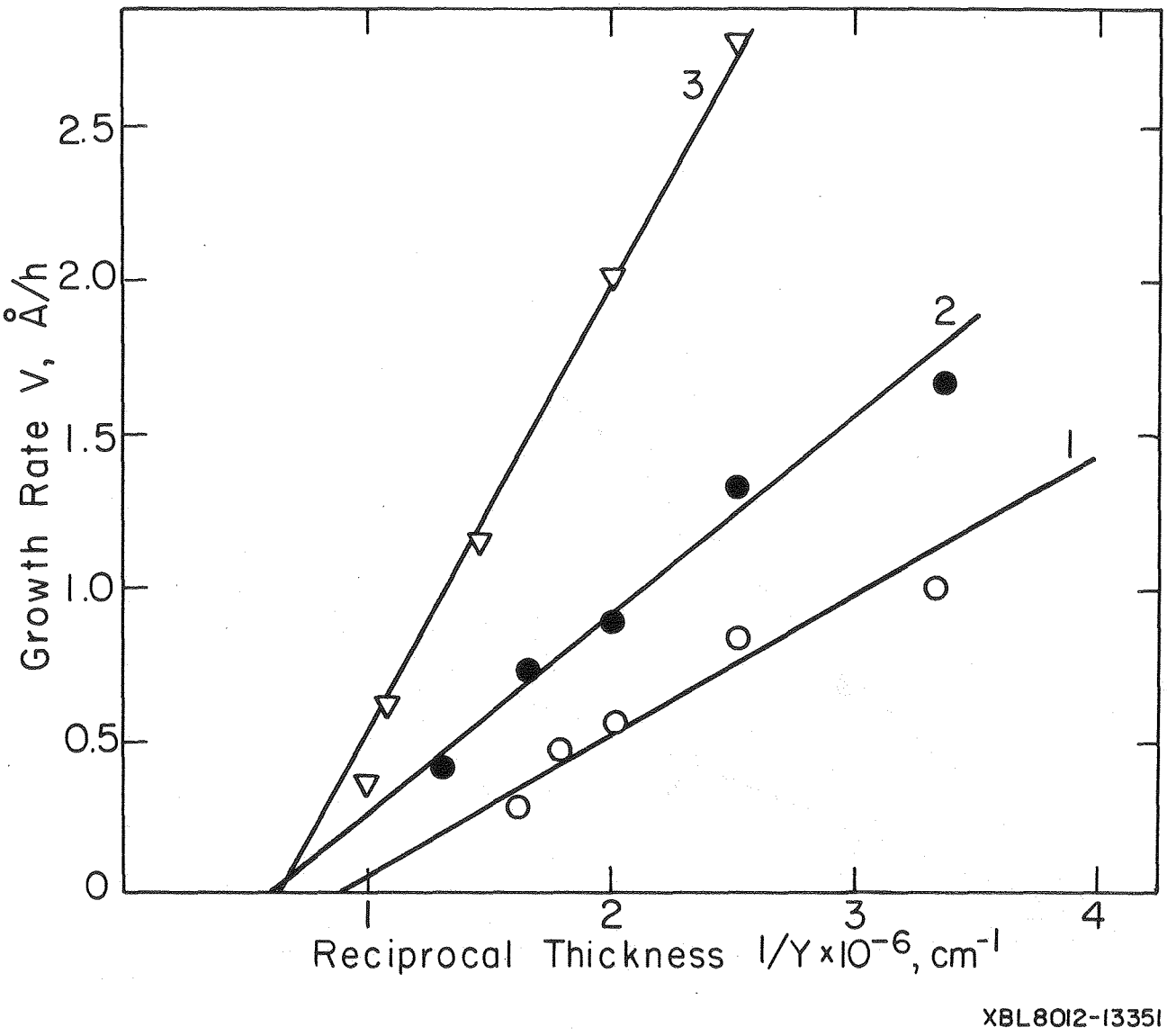
Growth Rate V, Å/h
0
0.5
1.0
1.5
2.0
2.5
1
2
3
4
Reciprocal Thickness 1/Y x10⁻⁶, cm⁻¹
3
2
1
XBL8012-13351

Figure 9

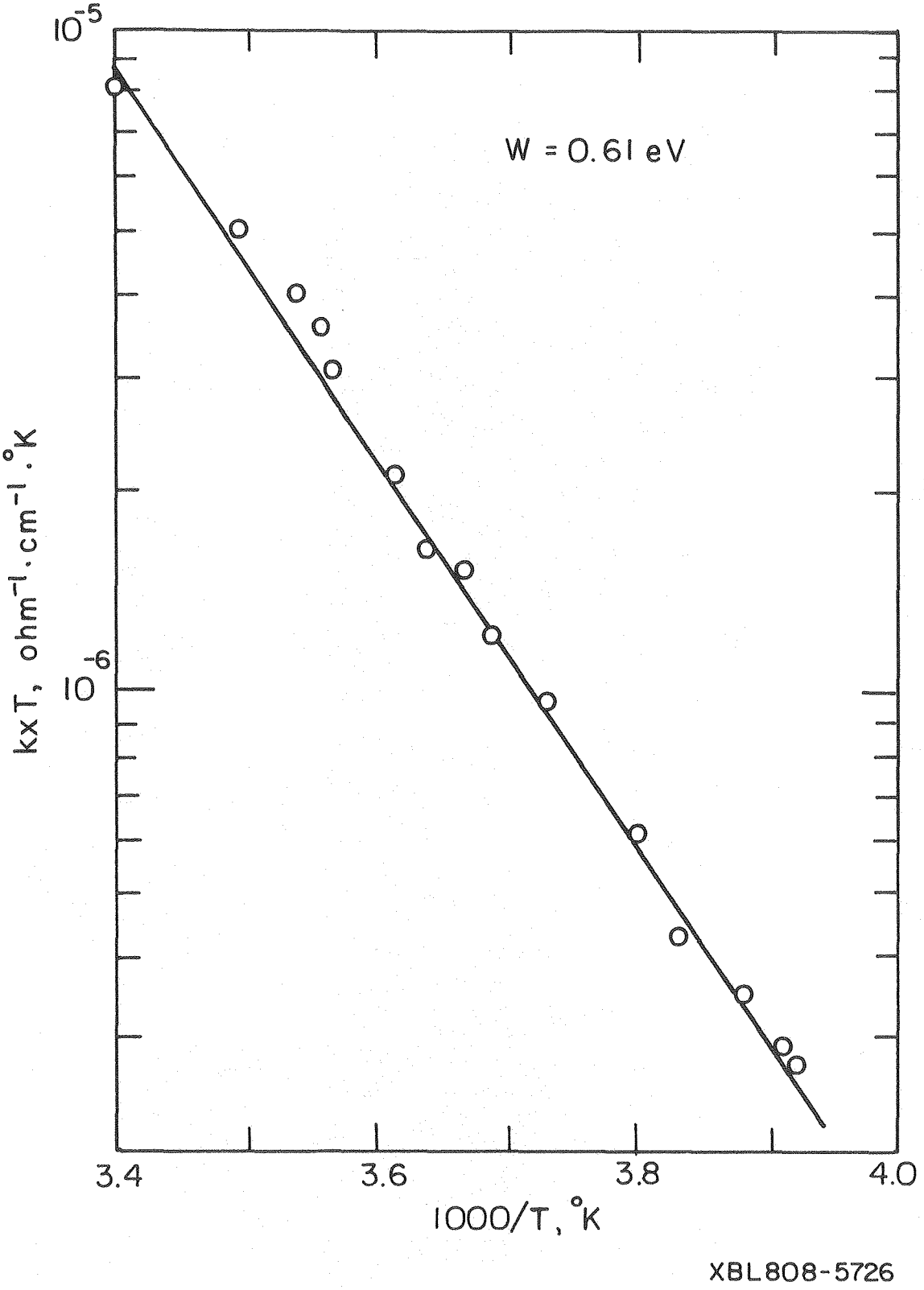

Figure 10

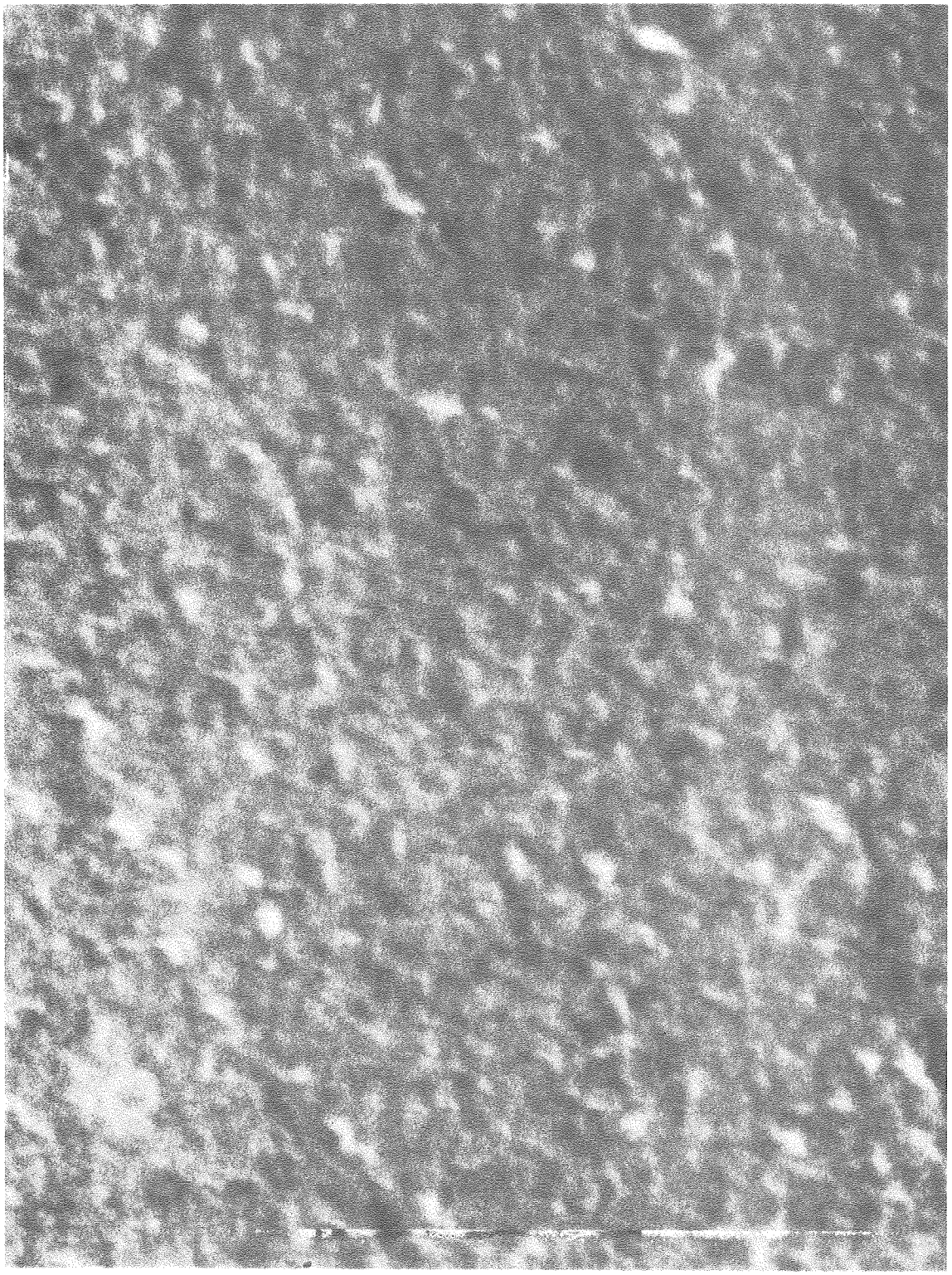

Figure 11

XBB 800-11290

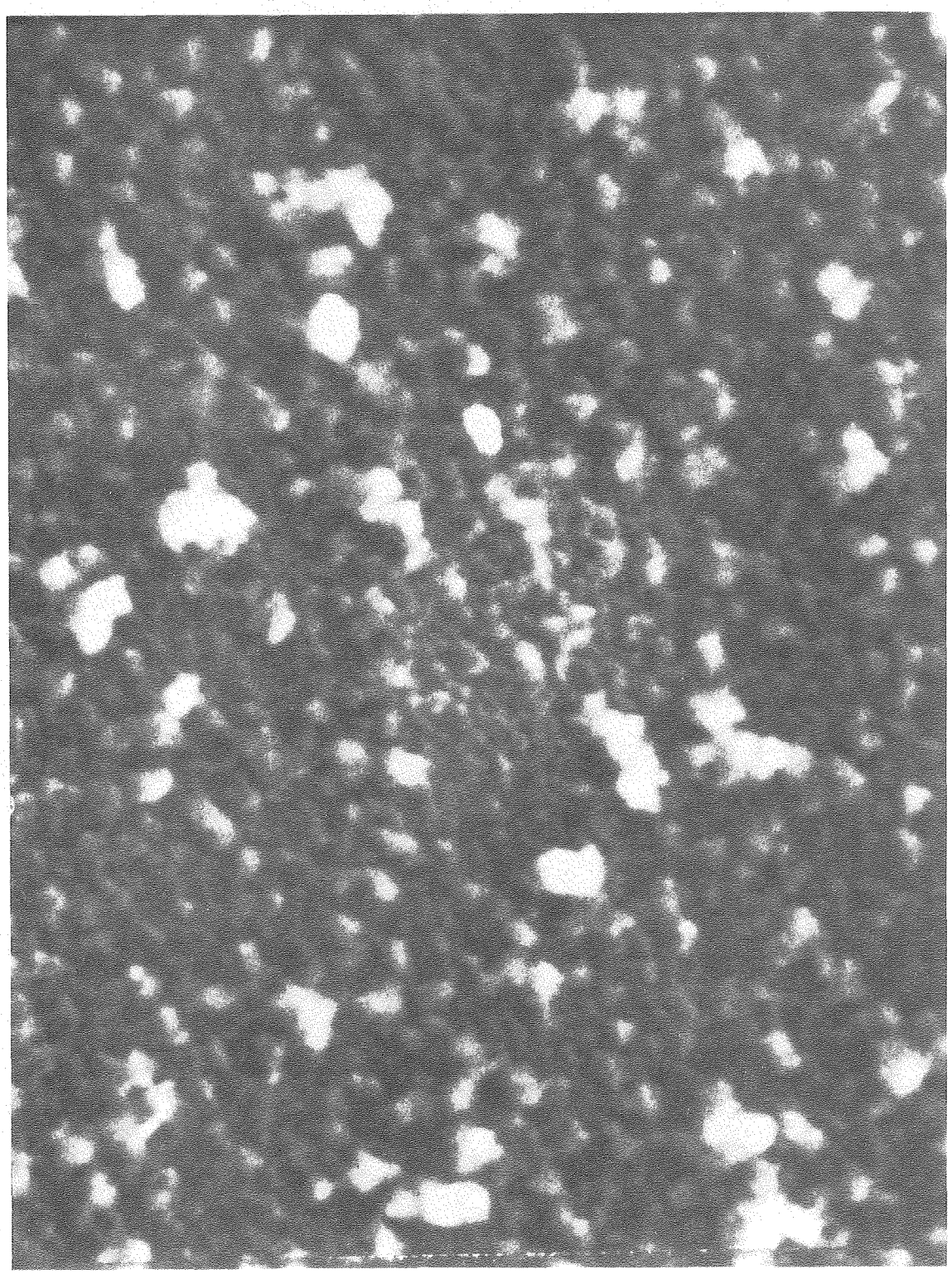

Figure 12

XBB 811-197

Figure 13

XBB 800-14890

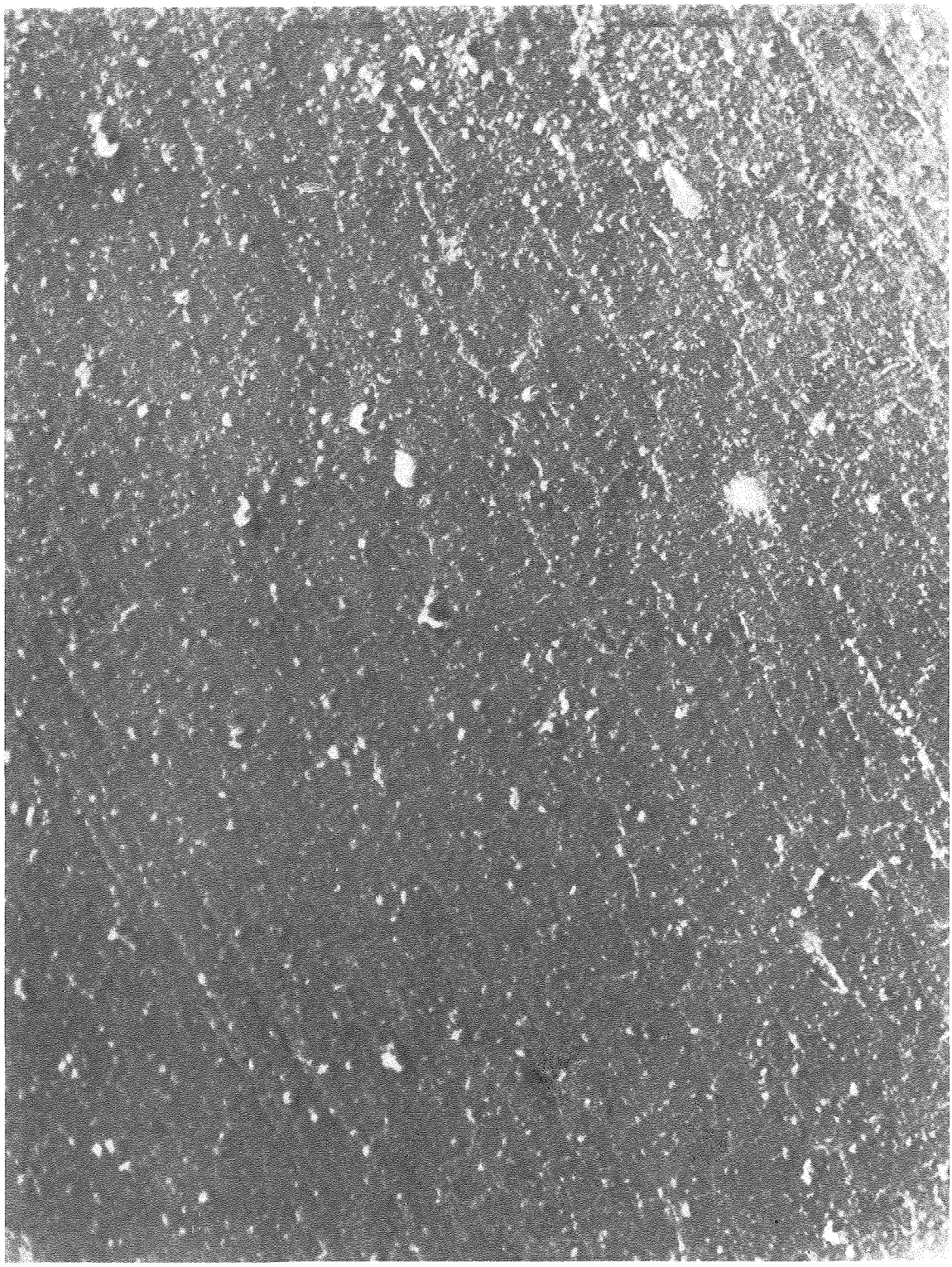

Figure 14

XBB 800-14892

Figure 15

XBB 800-14896

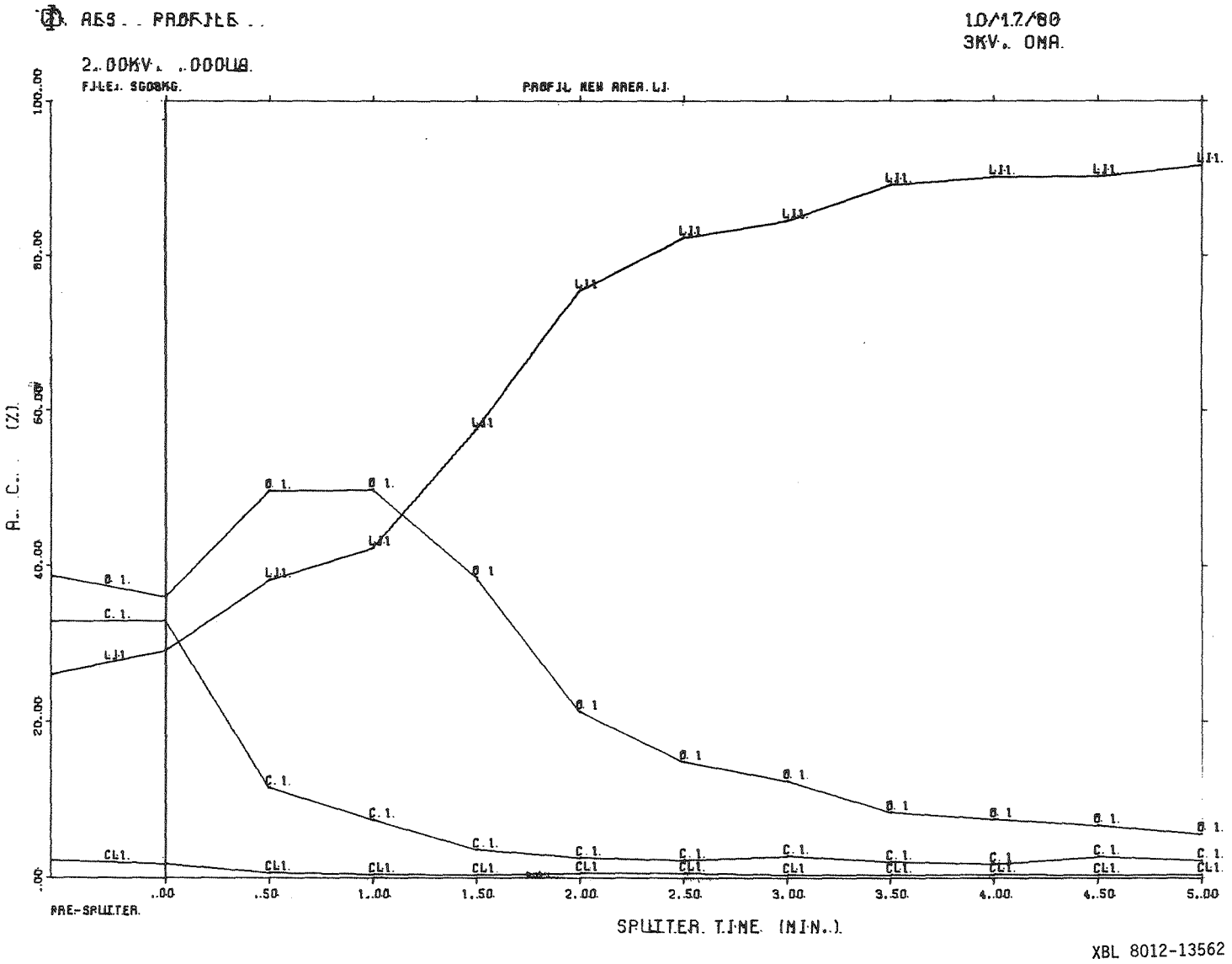
AES . . PROFILE . .
10/12/80
3KV. 0MA.
2..00KV. ..000UA.
FILE: SG00KG.
PROFIL MEN AREA.LJ.
A.. C.. (Z).
100.00
80.00
60.00
40.00
20.00
.00
PRE-SPLITTER.
..00
..50
1..00
1.50
2.00
2.50
3.00
3.50
4..00
4.50
5.00
SPLITTER. TIME. (MIN.).
XBL 8012-13562

Figure 16